

Measurement of the $6S \rightarrow 7S$ $M1$ transition in cesium with the use of crossed electric and magnetic fields

S. L. Gilbert, R. N. Watts, and C. E. Wieman

Department of Physics, University of Michigan, Ann Arbor, Michigan 48109

(Received 21 June 1983; revised manuscript received 4 August 1983)

The forbidden $6S \rightarrow 7S$ magnetic dipole transition amplitude in cesium has been measured by laser spectroscopy of an atomic beam in crossed electric and weak magnetic fields. The $M1$ amplitude was determined by observing the change in the transition rate caused by interference with a Stark-induced $E1$ amplitude. The result for the nuclear-spin-independent amplitude is $-42.10(80) \times 10^{-6} \mu_B$; the result for the nuclear-spin-dependent amplitude is $7.59(55) \times 10^{-6} \mu_B$. These values disagree with earlier measurements but they are in good agreement with theory. The experimental approach is well suited to measuring parity-violating neutral-current interactions.

INTRODUCTION

The $6S$ -to- $7S$ magnetic dipole ($M1$) transition in cesium has received considerable attention recently because of its role in the study of parity violation in atoms. However, the mechanism responsible for this very small transition amplitude ($\sim 10^5$ times smaller than an allowed $M1$ transition) has remained unclear. For some time the dominant mechanism was thought^{1,2} to be the fourth-order product of the interconfiguration and spin-orbit interactions. Recent more accurate calculations^{3,4} of this product, however, have shown that it is at least an order of magnitude smaller than the experimental value measured by Bouchiat and Pottier⁵ and later by Hoffnagle *et al.*⁶ Stimulated by this, Flambaum *et al.*⁴ proposed that a third-order contribution to the $M1$ amplitude would exist and calculated its size. However, this value was nearly a factor of 2 larger than the experimental value, as discussed in Appendix A. Several authors^{2,3,6} have pointed out that, in addition to this nuclear-spin-independent component of the amplitude, the off-diagonal hyperfine interaction would give rise to a smaller nuclear-spin-dependent component. There was even poorer agreement between theoretical and experimental values for this component.⁶ This was particularly puzzling because the calculation of this quantity is straightforward and can be directly related to well-known hyperfine splittings.

We report here the measurement of both components of the $M1$ amplitude using a new technique which yields higher sensitivity than previously possible and avoids a number of sources of systematic error which may have affected earlier work. Our results resolve the previous disagreements between theoretical predictions and experimental values. The experimental technique used has considerable promise for studying parity-violating neutral-current effects in atoms. We conclude with a brief discussion of this future application.

The experimental approach employs the interference between the $M1$ amplitude and a larger electric dipole ($E1$) amplitude. The measurement of a small amplitude by observing its interference with a larger known amplitude has been applied to a variety of problems but was first dis-

cussed in this context by the Bouchiats.² Neglecting parity-violating effects, only $M1$ or higher multipole transitions can take place between states of the same parity in an unperturbed atom. The application of a weak dc electric field, however, creates a small admixture of states of opposite parity which gives rise to a "Stark-induced" $E1$ transition amplitude. They pointed out that this amplitude can interfere with both the $M1$ amplitude and a parity-violating $E1$ amplitude arising from neutral-current interactions. Thus the measurement of these two amplitudes via this interference involves very similar experimental considerations. In the absence of a magnetic field, both of these interference terms can create a polarization of the excited state but cannot affect the transition rate.² A number of impressive measurements of small $M1$ (see Refs. 5,7,8) and parity-violating $E1$ amplitudes^{9,10} have been made by determining this polarization. However, such measurements suffer from a loss in sensitivity because the state polarization cannot be measured directly. It must be inferred from the degree of polarization of light absorbed or emitted in a transition from the excited state. In general this will be less than the atomic polarization and can be a source of systematic error in determining the amplitude of interest. Our method avoids these difficulties because the interference is manifested as a direct contribution to the transition rate. This requires that the Zeeman sublevels be resolved. We achieve this by using narrowband laser light to excite transitions in an atomic beam in the presence of a weak magnetic field.

The concept of such interference terms affecting the transition rate when a magnetic field is present has been discussed a number of times, though never experimentally demonstrated. The idea was implicit in the experiment to search for parity violation in hydrogen proposed by Lewis and Williams.¹¹ Following that, it was discussed explicitly by several authors in the context of possible techniques for the measurement of parity violation in heavy atoms.^{12,13} Recently Bouchiat and Poirier¹⁴ have extended that discussion to the closely related problem of measuring weak $M1$ amplitudes. All these proposed methods require magnetic fields on the order of 1 kG resulting in a complex relationship between the data and the amplitudes

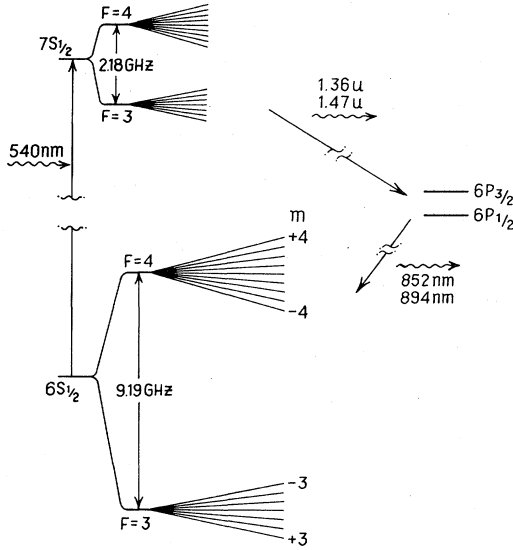


FIG. 1. Cesium energy-level diagram showing hyperfine and weak field Zeeman structure of $6S$ and $7S$ states.

of interest. A significant difference between these proposals and our experiment is that we require only tens of Gauss. This small field makes the interpretation of the data quite simple, as we will discuss, and substantially reduces a number of possible systematic errors.

THEORY

The use of crossed atomic and laser beams provides inherently narrow transition linewidths with little background. An additional experimental consideration however is the configuration of the magnetic (\vec{B}), the static (\vec{E}), and oscillating ($\vec{\epsilon}$) electric fields. The magnetic field, if weak, causes the Zeeman sublevels to split according to $\Delta E/h = mg_F \mu_B B$, where m is the quantum number for the z component of the total angular momentum F . For transitions between states with the same values of \vec{L} and \vec{J} the resulting spectrum is dramatically different depending on whether \vec{E} is parallel or perpendicular to $\vec{\epsilon}$. For the parallel case the selection rules for the Stark-induced transitions are $\Delta F=0$ and $\Delta m=0$. In the weak-magnetic-field limit the energies of all the $\Delta m=0$ transitions remain the same because the initial and final values of F , and hence

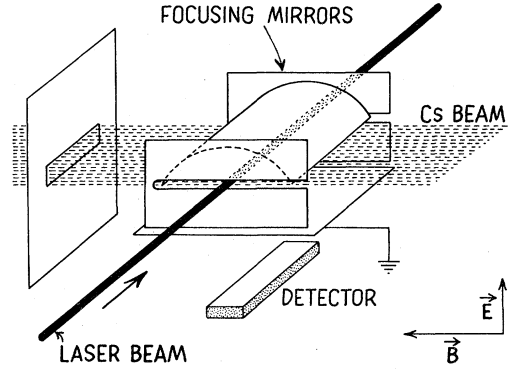


FIG. 2. Schematic of excitation region. Magnetic field coils and the wire mesh E field plates below and above the plane of intersection of the two beams are not shown.

g_F , are the same. Thus only a single line is observed and the interference terms do not contribute to the transition rate. Only in intermediate and high magnetic fields do the ground- and excited-state Zeeman levels shift differently allowing transitions to different Zeeman sublevels to be resolved.

For the case \vec{E} perpendicular to $\vec{\epsilon}$ the selection rules are $\Delta F=0, \pm 1$, and $\Delta m=0, \pm 1$. This gives rise to a multiplet structure even in the weak-field regime. Because the different lines in the multiplet involve transitions between different Zeeman sublevels, the transition rate for any given line will contain a contribution from the interference term. Thus the necessary resolution is achieved in quite a weak (tens of Gauss) magnetic field which has the advantages previously mentioned as well as simplifying the experimental apparatus.

We shall illustrate the other features of the experimental technique by considering in more detail the $6S \rightarrow 7S$ hyperfine transitions in cesium which were studied. These can be seen on the cesium energy level diagram in Fig. 1. Although other possible field configurations could be used, in particular, \vec{E} along the laser propagation direction, in the interest of brevity we shall limit our discussion to the configuration shown in Fig. 2. The static electric and magnetic fields are perpendicular and the transition is excited by laser light propagating perpendicularly to \vec{E} and \vec{B} , with $\vec{\epsilon}$ parallel to \vec{B} .

The Stark-induced $E1$ amplitude for a transition from an initial state $6S_{Fm}$ to a final state $7S_{F'm'}$ is given by

$$\begin{aligned} \mathcal{A}_{Fm}^{F'm'}(E1) &= \sum_n \left[\frac{\langle 7S_{F'm'} | -e\vec{\epsilon} \cdot \vec{r} | nP \rangle \langle nP | -e\vec{E} \cdot \vec{r} | 6S_{Fm} \rangle}{E_{6S} - E_{nP}} + \frac{\langle 7S_{F'm'} | -e\vec{E} \cdot \vec{r} | nP \rangle \langle nP | -e\vec{\epsilon} \cdot \vec{r} | 6S_{Fm} \rangle}{E_{7S} - E_{nP}} \right] \\ &= \beta E \epsilon C_{Fm}^{F'm'}, \end{aligned} \quad (1)$$

where $C_{Fm}^{F'm'}$ is proportional to the usual Clebsch-Gordan coefficient and is tabulated in Appendix B. The vector transition polarizability β , introduced in Ref. 2, is given by

$$\beta = \frac{1}{6} \sum_n \left[\langle 7S_{1/2} || r || nP_{1/2} \rangle \langle nP_{1/2} || r || 6S_{1/2} \rangle \left[\frac{1}{E_{7S} - E_{nP_{1/2}}} - \frac{1}{E_{6S} - E_{nP_{1/2}}} \right] \right. \\ \left. + \frac{1}{2} \langle 7S_{1/2} || r || nP_{3/2} \rangle \langle nP_{3/2} || r || 6S_{1/2} \rangle \left[\frac{1}{E_{7S} - E_{nP_{3/2}}} - \frac{1}{E_{6S} - E_{nP_{3/2}}} \right] \right]. \quad (2)$$

The $M1$ amplitude for this transition is given by

$$\mathcal{A}_{Fm}^{F'm'}(M1) = \langle 7S_{F'm'} | \vec{\mu} \cdot \vec{B} | 6S_{Fm} \rangle. \quad (3)$$

The selection rules are $\Delta F = 0, \pm 1$ and $\Delta m = \pm 1$. This amplitude can be written as the sum of two terms proportional to M and $(F - F')M_{\text{hf}}$, respectively, where M is the nuclear-spin-independent component and M_{hf} is the nuclear-spin-dependent component. This gives

$$\mathcal{A}_{Fm}^{F'm'}(M1) = [M + (F - F')M_{\text{hf}}] (C_{Fm}^{F'm'}) \quad (\Delta m = +1) \\ \text{and} \quad (4)$$

$$\mathcal{A}_{Fm}^{F'm'}(M1) = [M + (F - F')M_{\text{hf}}] (-C_{Fm}^{F'm'}) \quad (\Delta m = -1).$$

For each transition between particular Zeeman sublevels, $6S_{Fm} \rightarrow 7S_{F'm'}$, the transition rate I , is the square of the sum of the $E1$ and $M1$ amplitudes,

$$I_{Fm}^{F'm'} = |\mathcal{A}(E1) + \mathcal{A}(M1)|^2 \\ = |\mathcal{A}(E1)|^2 + 2\mathcal{A}(E1)\mathcal{A}(M1) + |\mathcal{A}(M1)|^2. \quad (5)$$

For the case we are interested in $|\mathcal{A}(M1)| \ll |\mathcal{A}(E1)|$ so we can neglect the $|\mathcal{A}(M1)|^2$ term. Then from Eqs. (1) and (4) we can write

$$I_{F,m'\pm 1}^{F',m'\pm 1} = \epsilon^2 \{ \beta^2 E^2 \mp 2\beta E [M + (F - F')M_{\text{hf}}] \} \\ \times (C_{F,m'\pm 1}^{F',m'\pm 1})^2. \quad (6)$$

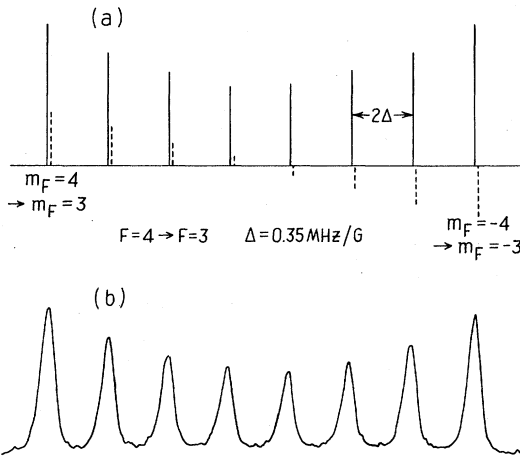


FIG. 3. (a) Theoretical spectrum. The solid lines are the $|\mathcal{A}(E1)|^2$ contributions while the dashed lines are the $2\mathcal{A}(E1)\mathcal{A}(M1)$ contributions on an expanded vertical scale. The dashed lines have been shifted slightly to the right for ease of viewing. Actually both lines occur at the same frequency and the observed intensity will be the sum of the two contributions. (b) Scan of $6S_{F=4} \rightarrow 7S_{F=3}$ transition with $B = 100$ G.

The notable feature of this equation is that the transition rate contains a pure Stark-induced $E1$ term, $\beta^2 E^2$, plus an $E1$ - $M1$ interference term—the sign of which depends on E and Δm .

Using Eq. (6) and the fact $g_{F=4} = -g_{F=3}$, we can now obtain the spectrum for the three Zeeman multiplets of interest.

$6S_{F=4} \rightarrow 7S_{F=3}$. The spectrum contains eight lines where each line strength $R(i)$ is given by

$$R(i) = I_{4,i-1}^{3,i} + I_{4,i}^{3,i-1}, \quad i = -3 \text{ to } +4. \quad (7)$$

The two outermost lines of the multiplet each involve only a single transition ($m = 4 \rightarrow 3$ and $m = -4 \rightarrow -3$, respectively) while each of the other six lines is the sum of a $\Delta m = +1$ and a $\Delta m = -1$ transition. The calculated spectrum is shown in Fig. 3(a). The actual rate for each line in the figure is the sum of the pure $E1$ contribution (solid line) and the $E1$ - $M1$ interference (offset dashed line on an expanded vertical scale).

$6S_{F=3} \rightarrow 7S_{F=4}$. This has a nearly identical spectrum to the $F=4 \rightarrow 3$ transition. The only difference is that the interference terms are now proportional to $M - M_{\text{hf}}$ instead of $M + M_{\text{hf}}$.

$6S_{F=4} \rightarrow 7S_{F=4}$. For this transition all the $\Delta m = +1$ transitions are shifted up in frequency by $(0.35 \text{ MHz/G})B$ while all the $\Delta m = -1$ transitions are shifted down by this amount. The spectrum thus contains only two lines with their rates given by

$$R(+)= \sum_{m=-4 \rightarrow +3} I_{4,m}^{4,m+1} = \frac{15}{8} \epsilon^2 (\beta^2 E^2 + 2\beta E M), \quad (8)$$

$$R(-)= \sum_{m=-3 \rightarrow +4} I_{4,m}^{4,m-1} = \frac{15}{8} \epsilon^2 (\beta^2 E^2 - 2\beta E M).$$

This analysis used the weak-field limit for the Zeeman effect which assumes no mixing of different hyperfine states by the magnetic field. In the field regime of interest this mixing can be accurately calculated using second-order perturbation theory. We find its effect is to change the relative transition strengths slightly from the weak-field limit. For a typical field of 40 G the changes range between 0% and 3.4% for the various lines of the multiplets discussed. However, for the spectral lines measured in this paper, the size of the change is unimportant because the corresponding $E1$ and $M1$ amplitudes are affected by exactly the same amount. Thus the ratio of the two amplitudes, which is the quantity of interest, is independent of the mixing of the hyperfine states.

For all three hyperfine transitions the interference terms are odd under reversal of \vec{E} , \vec{B} , and the changing of the excitation frequency to the opposite multiplet component, providing a simple experimental way to isolate and mea-

sure them. The experiment consists of carrying out these reversals and detecting the resulting fractional modulation in the transition rate. In principle any single reversal would be sufficient but in practice the extra reversals are valuable for eliminating systematic errors.

EXPERIMENT

We have used this technique to measure the ratios of the magnetic dipole amplitude to the Stark-induced amplitude β , for the $6S_{F=3} \rightarrow 7S_{F=4}$, the $6S_{F=4} \rightarrow 7S_{F=3}$, and $6S_{F=4} \rightarrow 7S_{F=4}$ transitions in cesium. The $F=3 \rightarrow 4$ and $F=4 \rightarrow 3$ transitions were measured, then the apparatus was modified slightly and all three transitions measured. In a previous work¹⁵ we determined the absolute value of β .

The experiment is shown schematically in Fig. 2. A narrow-band dye-laser beam intersects a collimated beam of atomic cesium in a region of perpendicular electric and magnetic fields. The $6S \rightarrow 7S$ transition rate is monitored by observing the 850- and 890-nm light emitted in the $6P_{3/2,1/2} \rightarrow 6S_{1/2}$ step of the $7S$ decay. The dye laser is a Spectra-Physics model No. 380 dye laser with homemade frequency and amplitude stabilizers. The output power is typically 500 mW with a linewidth of ~ 100 KHz. The cesium beam, which is produced by a two-stage oven to reduce the dimer fraction, is collimated to 0.015 rad. The 2.5-cm-long region of intersection of the two beams is imaged onto a silicon photodiode by a 5-cm-long gold-coated cylindrical mirror with flat ends. The scattered 540-nm light is blocked by a colored glass cutoff filter in front of the detector. This filter is coated with an optically transparent conductive coating. Fine wire mesh was placed above and below the interaction region and the electric field was produced by applying voltage (typically 1.6 KV) to the upper mesh and grounding the lower. For the first run the mesh spacing was ~ 0.5 cm while for the second a new collector was used with a ~ 0.6 -cm spacing. A 40-G magnetic field is provided by a 25-cm-diam Helmholtz pair.

Data was obtained by locking the laser frequency to the peak of a particular line of the multiplet and reversing the electric field every 0.25 sec. During each half cycle of electric field the detector output was integrated, digitized, and stored by a Digital Equipment Corporation model No. PDP-11 computer. For each of the three hyperfine transitions data was taken on the extreme high- and low-frequency lines of the Zeeman multiplets as these provide the largest signals. This was done for both directions of magnetic field providing a total of four data sets for each hyperfine line. At 1–2-min intervals during these measurements the electric field was set to zero to determine the baseline for the transition. To test for any asymmetry in the reversal of \vec{E} , data was also taken at zero magnetic field for laser frequencies both on and well off the transitions.

To test for frequency-dependent background signals the laser frequency was scanned over the transitions both with and without magnetic field and the spectra recorded. One such scan with a rather large magnetic field is shown in Fig. 3(b). The 14 MHz linewidth is due to the residual

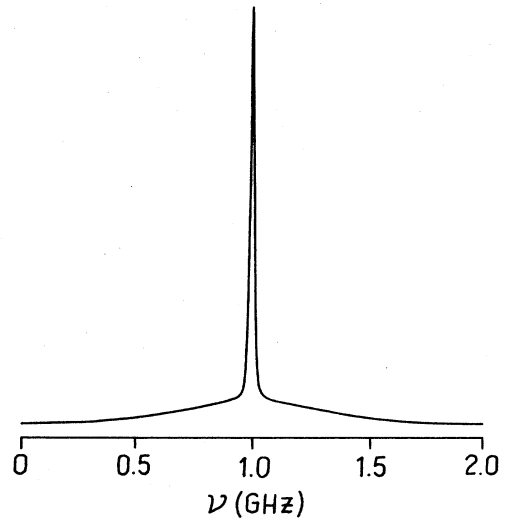


FIG. 4. Scan of transition with $B=0$.

Doppler shift from the cesium beam divergence.

In order to obtain an absolute value for the $M1$ amplitude it is necessary to know the dc electric field. We determined this by measuring the Stark shift of the $6S_{F=4} \rightarrow 7S_{F=4}$ transition as described in Ref. 15. Once the Stark shift was known the field was found using the polarizability given in that reference.

DATA ANALYSIS AND RESULTS

The data analysis primarily consisted of taking the difference between the positive electric field and negative electric field transition rates and dividing it by the average rate. From Eqs. (6)–(8), this is simply

$$\frac{\Delta R}{R} = \frac{\pm 4\beta E M_{\text{eff}}}{\beta^2 E^2}, \quad (9)$$

where M_{eff} is $M + M_{\text{hf}}$, $M - M_{\text{hf}}$, and M , for the three transitions studied. However, considerable additional effort was devoted to determining and correcting for possible systematic errors.

First we considered systematic errors which could have been introduced by various background signals. The cesium oven and, to a lesser extent, the scattered laser light gave appreciable background signals which were independent of laser frequency. The only effect of these signals on our measurement was to cause a slow uniform drift in the detector zero level, typically corresponding to 1% of the transition rate per minute. This drift was determined from the $E=0$ data and did not introduce a significant uncertainty.

The scans of laser frequency over the transition showed a broad frequency-dependent background signal centered on the atomic transition frequency. This can be seen in Fig. 4. We ascribe this signal to an isotropic background gas of cesium in the interaction region. The line shape was accurately determined from the spectra taken with $B=0$. The background pedestal could be fitted well by a 575-MHz-wide Gaussian curve. The height varied between 0.040(2) and 0.067(2) times the height of the 14-

MHz-wide peak for the different runs. This pedestal contributes to both the average ($\beta^2 E^2$) transition rate and the $E1$ - $M1$ modulation. The contribution to the modulation is considerably diluted over that given in Eq. (9) because the linewidth is much broader than the Zeeman splitting. Using the measured line shape we calculated the correction needed because of the presence of the pedestal (11–26%). We do not observe any other frequency-dependent background—in particular, that due to molecular cesium which was significant in the work discussed in Refs. 5 and 6.

A number of possible systematic errors associated with the field reversals were also checked. The use of three independent mechanisms to reverse the sign of the interference term greatly reduces such errors but a number of independent experimental tests were also made. These included tests of the following: (1) detector sensitivity depending on direction of \vec{E} or \vec{B} , (2) imperfect \vec{B} reversal, (3) imperfect \vec{E} reversal, (4) error due to \vec{e} not perfectly linearly polarized perpendicular to \vec{E} , (5) misalignment of \vec{B} with respect to \vec{E} and \vec{e} , and (6) pickup of \vec{E} field-switching transients. None of these sources were found to be significant at the level of the experimental uncertainty except the \vec{E} field switching transients. These were determined from the modulation signal measured when no laser light was present. It was found to be $\sim 9\%$ of the interference term. Since this spurious signal is always the same sign, its effect averages to zero when the data for different directions of magnetic field and different lines of the multiplet are averaged.

In order to obtain an absolute value for the $M1$ amplitude from the ratio given by Eq. (9) it is necessary to know E . From the Stark shift of the $6S_{F=4} \rightarrow 7S_{F=4}$ transition we obtained 2934(15) V/cm for the first data run. For the second run, values of E between 2661(10) and 2997(10) V/cm were used. The values obtained from the Stark shift agreed well with less accurate ($\sim 5\%$) values calculated by dividing the applied voltage by the mesh separation. The dependence of the transition line shape on electric field also provides a test of the field uniformity. We find that the 14-MHz linewidth is changed by less than 1% in going from 625 to 5000 V/cm while the line center shifts 17.5 MHz [$\Delta\nu = 0.71$ Hz (V/cm) $^{-2}$ from Ref. 15]. This implies that any spatial variation of the field strength is substantially less than 1%.

In Fig. 5 we present the fractional changes in the transition rate observed for the different lines. We have put in corrections for the pedestal and the electric field transients. For display purposes we have normalized all the data to a field of 2997 V/cm. Comparing across each row one can see the expected sign changes. Also the agreement in the magnitudes provides further confirmation that all the reversals are working as planned.

From this data and Eq. (9) we obtain from the first run in V/cm

$$\frac{M - M_{\text{hf}}}{\beta} = -35.80(75), \quad \frac{M + M_{\text{hf}}}{\beta} = -24.93(65),$$

and for the second run in V/cm

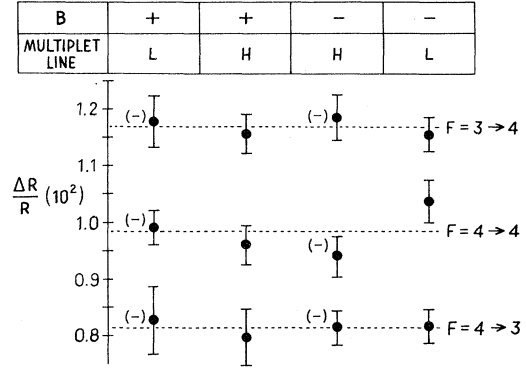


FIG. 5. Fractional changes in transition rates. Direction of the magnetic field is indicated by the + and - while the H and L indicate the multiplet line. The highest frequency line is labeled H and the lowest L . The ΔR 's in the first and third columns were negative, as indicated. Each dotted line is the average of the four points in that row. All the data was normalized to 2997 V/cm.

$$\frac{M - M_{\text{hf}}}{\beta} = -34.59(80), \quad \frac{M + M_{\text{hf}}}{\beta} = -24.10(70),$$

$$\frac{M}{\beta} = -29.43(62),$$

where this value for M/β is based on only the $F=4 \rightarrow 4$ data.

In Table I we combine these results and compare with earlier measurements. With the exception of the value for $(M - M_{\text{hf}})/\beta$ our results disagree with the earlier measurements. These earlier measurements of M/β were made using $\Delta F=0$ transitions while for our first data run we derived this quantity from $\Delta F=+1$ and -1 transitions. The disagreement between these led us to speculate that perhaps, contrary to Eq. (4), there was some unsuspected $M1$ component which contributed equally to the $\Delta F \neq 0$ lines and did not contribute to the $\Delta F=0$ transitions. However, the agreement between the value of M/β we obtained from the $\Delta F=+1$ and -1 transitions [$-29.83(40)$ V/cm] and the value we subsequently obtained from the $F=4 \rightarrow F=4$ transition rules out such an idea.

Using $\beta = 26.6(4)a_0^3$ as discussed in Appendix A we obtain

$$M = -42.10(80) \times 10^{-6} \mu_B,$$

$$M_{\text{hf}} = 7.59(55) \times 10^{-6} \mu_B.$$

Considering the uncertainty in the calculation, the value for M is in agreement with the recent value of -63×10^{-6}

TABLE I. Measurements of $M1$ Amplitudes

	Ref. 5	Ref. 6	This work
$\frac{M}{\beta}$ (V/cm)	-23.2(1.3)	-26.2(1.7)	-29.73(34)
$\frac{M - M_{\text{hf}}}{\beta}$ (V/cm)		-34.3(2.1)	-35.21(56)
$\frac{M_{\text{hf}}}{M}$		-0.31(3)	-0.180(13)

calculated by Flambaum, Khriplovich, and Sushkov⁴ for the contribution due to the product of first-order interconfiguration interaction and second-order off-diagonal spin-orbit interaction.

M_{hf} arises from the mixing of states of different n by the hyperfine interaction. Hoffnagle⁶ has shown it can simply be expressed as (theory)

$$M_{\text{hf}} = \frac{(\Delta w_{6S} \Delta w_{7S})^{1/2}}{w_{6S} - w_{7S}} \mu_B = 8.04 \times 10^{-6} \mu_B,$$

where Δw_{6S} and Δw_{7S} are the accurately known hyperfine splittings of the 6S and 7S states.¹⁶ This value is expected to be quite accurate, and is in good agreement with our measured value.

EXTENSIONS OF THE TECHNIQUE

The experimental approach of crossed beams in a weak magnetic field can also be used to measure the parity-violating $E1$ amplitude [$\mathcal{A}(E1_{\text{pv}})$] arising from neutral-current mixing of the S and P states. As mentioned earlier this interferes with the Stark-induced amplitude in a manner similar but not identical to the $M1$ amplitude. For the field configuration we have discussed, one significant difference, which was mentioned in the Bouchiat early work,² is that the parity-violating mixing matrix element is imaginary relative to the Stark mixing matrix element. Thus no interference will be present for linearly polarized light. This can be remedied by using elliptically polarized light, $\vec{\epsilon} = \vec{\epsilon}_{\perp} + i\vec{\epsilon}_{\parallel}$, where the \perp and \parallel are with respect to \vec{E} . Now $i\vec{\epsilon}_{\parallel}$ creates a parity-violating amplitude which has the same phase and hence interferes with the Stark-induced amplitude. Carrying through a similar analysis as before (including the mixing of hyperfine states) for the $6S_{F=4} \rightarrow 7S_{F=3}$ transition one obtains the same Clebsch-Gordan coefficients and the same spectrum as for the $M1$ case shown in Fig. 3(a). The only difference is that now the vertical scale for the interference terms is proportional to $(\epsilon_{\parallel} E \beta) [\epsilon_{\parallel} \mathcal{A}(E1_{\text{pv}})]$. Like the $M1$ case the interference terms change sign with a reversal of \vec{E} , \vec{B} , and multiplet component. However, unlike the $M1$ case they do not change sign if the laser light propagation direction is reversed¹⁷ and they have the additional signature that they change sign when the "handedness" of the light is reversed ($i\epsilon_{\parallel} \rightarrow -i\epsilon_{\parallel}$). It might also be noted that the ratio between interference and pure Stark-induced contributions to the transition rate can be enhanced by making $\epsilon_{\parallel}/\epsilon_{\perp} > 1$.

The apparatus previously described is thus well suited to measure this parity-violating term. Besides the use of elliptically polarized light, the only significant change needed is the addition of a power buildup interferometer cavity of the type we have previously used.^{15,16} This provides ~ 150 times more laser power in the interaction region. Because the signal to noise ratio is limited entirely by detector noise this should give a corresponding improvement in the signal-to-noise ratio while suppressing the $E1$ - $M1$ interference. For a parity-violating amplitude of the size measured by Bouchiat *et al.*¹⁰ ($\sim 10^{-4}$ times the $M1$), such a signal-to-noise ratio would allow a one standard-deviation measurement of $E1_{\text{pv}}$ with an integrat-

ing time on the order of 10 min.

The apparatus has potential for considerable future improvement. For the measurement of $M1$ amplitudes the addition of a traveling-wave ring buildup cavity would improve the signal-to-noise ratio by ~ 100 . Also the use of an optically pumped atomic beam would provide a 16-fold increase in signal for measurements of both the $\mathcal{A}(M1)$ and $\mathcal{A}(E1_{\text{pv}})$ amplitudes and eliminate the need for a magnetic field.

Note added in proof. We have learned that Bouchiat, Guena, and Pottier have recently remeasured M/β and measured M_{hf}/β , and they now obtain results in excellent agreement with ours.

ACKNOWLEDGMENTS

We are pleased to acknowledge the assistance of M. C. Noecker on this experiment and D. Kleppner for a critical reading of the manuscript. This work was supported by the National Science Foundation and in part by Research Corporation. One of us (R.N.W.) was supported by a University of Michigan Rackham Fellowship.

APPENDIX A: THE VALUE OF β

A certain amount of confusion has been caused by the value of the vector transition polarizability β used in Ref. 5. The quantity actually measured in that work was the value of M/β given in Eq. (13) of that reference and listed in our Table I. By using a value of 8.8(4) for the ratio of scalar to vector transition polarizability, $|\alpha/\beta|$, and a theoretical value of $(-305a_0^3)$ for α , they quoted an absolute value for M of $4.24(34) \times 10^{-5} |\mu_B|$. Subsequent measurements by Hoffnagle *et al.*⁶ and ourselves,¹⁶ and a remeasurement by Bouchiat *et al.*¹⁸ have obtained values for $|\alpha/\beta|$ of 9.91(11), 9.80(12), and 9.90(10), respectively. We have experimentally determined¹⁵ α to be $-263.7(27)a_0^3$. From the average of these results we take $|\alpha/\beta| = 9.9(1)$ and arrive at a value of $\beta = 26.6(4)a_0^3$. Using this value for β , the M/β given in Ref. 5 gives $M = 3.3(2) \times 10^{-5} \mu_B$ which is farther from the calculated value of $6.3 \times 10^{-5} \mu_B$ than the number originally quoted.

In the text we have taken care to only compare the measured ratios M_{eff}/β . To derive an absolute value for M and M_{hf} from our data we used $\beta = 26.6(4)a_0^3$ which was obtained as described.

APPENDIX B: $C_{Fm}^{F'm'}$ COEFFICIENTS

We find the $C_{Fm}^{F'm'}$ coefficients to be as follows:

$$C_{4,m'-1}^{4,m'} = +\frac{1}{8}[(5-m')(4+m')]^{1/2},$$

$$C_{4,m'+1}^{4,m'} = -\frac{1}{8}[(5+m')(4-m')]^{1/2},$$

$$C_{4,m'-1}^{3,m'} = +\frac{1}{8}[(4-m')(5-m')]^{1/2},$$

$$C_{4,m'+1}^{3,m'} = +\frac{1}{8}[(4+m')(5+m')]^{1/2},$$

$$C_{3,m'-1}^{4,m'} = -\frac{1}{8}[(3+m')(4+m')]^{1/2},$$

$$C_{3,m'+1}^{4,m'} = -\frac{1}{8}[(3-m')(4-m')]^{1/2},$$

$$C_{3,m'-1}^{3,m'} = -\frac{1}{8}[(4-m')(3+m')]^{1/2},$$

$$C_{3,m'+1}^{3,m'} = +\frac{1}{8}[(4+m')(3-m')]^{1/2}.$$

- ¹M. Phillips, Phys. Rev. **88**, 202 (1952).
- ²M. A. Bouchiat and C. Bouchiat, J. Phys. (Paris) **35**, 899 (1974); **36**, 493 (1975).
- ³D. V. Neuffer and E. D. Commins, Phys. Rev. A **16**, 1760 (1977).
- ⁴V. V. Flambaum, I. B. Khriplovich, and O. P. Sushkov, Phys. Lett. **67A**, 177 (1978).
- ⁵M. A. Bouchiat and L. Pottier, J. Phys. (Paris) Lett. **37**, L79 (1976).
- ⁶J. Hoffnagle, L. Ph. Roesch, V. Telegdi, A. Weis, and A. Zehnder, Phys. Lett. **85A**, 143 (1981); J. Hoffnagle, Ph.D. thesis, Swiss Federal Institute of Technology, Zurich, 1982 (unpublished).
- ⁷S. Chu, E. D. Commins, and R. Conti, Phys. Lett. **60A**, 96 (1977).
- ⁸W. Itano, Phys. Rev. A **22**, 1558 (1980).
- ⁹P. Bucksbaum, E. Commins, and L. Hunter, Phys. Rev. Lett. **48**, 607 (1982).
- ¹⁰M. A. Bouchiat, J. Guéna, L. Hunter, and L. Pottier, Phys. Lett. **117B**, 358 (1982).
- ¹¹R. R. Lewis and W. L. Williams, Phys. Lett. B **52**, 70 (1975).
- ¹²M. A. Bouchiat and L. Pottier, in Proceedings of the International Workshop on Neutral Current Interactions in Atoms, (Cargese, 1979), edited by W. L. Williams (unpublished); M. A. Bouchiat, M. Poirer, and C. Bouchiat, J. Phys. (Paris) **40**, 1127 (1979).
- ¹³P. Bucksbaum, in Proceedings of the International Workshop on Neutral Current Interactions in Atoms (Cargese, 1979), edited by W. L. Williams (unpublished). We are aware that an experiment along the lines discussed in this reference is being worked on by P. Drell and E. D. Commins (private communication).
- ¹⁴M. A. Bouchiat and M. Poirier, J. Phys. (Paris) **43**, 729 (1982).
- ¹⁵R. N. Watts, S. L. Gilbert, and C. E. Wieman, Phys. Rev. A **27**, 2769 (1983).
- ¹⁶S. L. Gilbert, R. N. Watts, and C. E. Wieman, Phys. Rev. A **27**, 581 (1983).
- ¹⁷M. A. Bouchiat and L. Pottier, *Laser Spectroscopy III*, edited by J. L. Hall and J. L. Carlsten (Springer, Berlin, 1977).
- ¹⁸M. A. Bouchiat, J. Guéna, L. Hunter, and L. Pottier, Opt. Commun. **45**, 35 (1983).